Simultaneous measurements of small angle x-ray scattering, wide angle x-ray scattering, and dielectric spectroscopy during crystallization of polymers

I. Šics,[a] A. Nogales, T. A. Ezquerra,[b] Z. Denchev,[c] and F. J. Baltá-Calleja
Instituto de Estructura de la Materia, C.S.I.C., Serrano 119, Madrid 28006, Spain

A. Meyer and R. Döhrmann
HASYLAB-DESY, Notkestrasse 85, 22603 Hamburg, Germany

(Received 4 October 1999; accepted for publication 14 December 1999)

A novel experimental setup is described which allows one to obtain detailed information on structural and dynamical changes in polymers during crystallization. This technique includes simultaneous measurements of small angle-wide angle x-ray scattering and dielectric spectroscopy (SWD). The capabilities of the technique have been probed by following in real time the crystallization process of a model crystallizable polymer: poly(ethylene terephthalate). By performing these experiments, simultaneous information from both, the amorphous and the crystalline phase is obtained providing a complete description of changes occurring during a crystallization process. The SWD technique opens up new promising perspectives for the experimental study of the relation between structure and dynamics in materials science. © *2000 American Institute of Physics.* [S0034-6748(00)01004-2]

I. INTRODUCTION

Crystallizable glassy polymeric materials may develop a certain level of crystallinity provided they are heated at temperatures above the glass transition temperature (T_g). In a typical isothermal crystallization process of an initially glassy polymeric system, crystallinity evolves in a sigmoidal fashion.[1–3] After an initial induction time, where no crystallinity development is observed, a primary crystallization process takes place where so-called spherulites or other morphological units grow until they completely fill the material.[1] Subsequently, a secondary crystallization regime is achieved where the crystallization rate is strongly reduced.

The spherulitic microstructure of semicrystalline polymers typically shows a distinct lamellar morphology consisting of stacks of laminar crystals intercalated by amorphous less ordered regions. The nature of the distribution of the crystalline regions may give rise to the appearance of different morphologies.[2–4] The lamellar stacks are characterized by the thickness of the crystals (l_c) and that of the amorphous layers (l_a). Both characteristic lengths define the long period as $L=l_a+l_c$ which can be experimentally determined through small angle x-ray scattering experiments (SAXS).[5] The crystalline fraction in the lamellar stacks is defined by $X_{cL}=l_c/(l_a+l_c)$ and can be estimated experimentally by SAXS measurements.[5] The overall crystalline fraction X_c can be estimated experimentally from wide angle x-ray scattering measurements (WAXS). In the case of space filling lamellar stack systems $X_{cL}=X_c$. Another important parameter which can be related with the microstructure is the integrated SAXS intensity defined by

$$Q \propto X_{cL}(1-X_{cL})(\rho_c-\rho_a)^2, \tag{1}$$

where ρ_c and ρ_a are the electronic densities of crystalline and amorphous phase, respectively. In order to obtain a precise information about the changes occurring in a polymeric system during crystallization, a real time experimental setup is of crucial importance.[6] As far as microstructure development is concerned, high intensity synchrotron radiation offers the possibility to perform simultaneous, real time SAXS and WAXS.[6] An improvement in the understanding of the correlation between microstructure and crystal development is obtained when both experiments are performed simultaneously.[7,8] Owing to the fact that both, SAXS and WAXS, are based on x-ray diffraction they provide information about the structure of the ordered regions at different length scales. At the same time, processes occurring in the amorphous fraction of the material are ''invisible'' for these techniques due to the absence of order. From the point of view of the amorphous phase, dielectric spectroscopy experiments (DS) have shown that, upon crystallization, its dynamics is strongly affected by the progressive development of the crystalline phase.[9–12] Hence, if one would monitor simultaneously, in real time, both, the microstructure development and the dynamic changes occurring in the amorphous phase, a more complete picture of the crystallization process could be obtained.

In this article we present, according to the foregoing concepts, the development of the experimental setup which has allowed one to perform simultaneous measurements of time resolved SAXS, WAXS, and DS. After a description of the experimental setup, the performance of the SAXS–WAXS–DS technique will be illustrated with the results ob-

[a]Permanent address: Riga Technical University, Institute of Polymer Materials, Latvia.
[b]Electronic mail: imte155@iem.cfmac.csic.es
[c]Permanent address: University of Sofia, Laboratory on Polymers, Bulgaria.

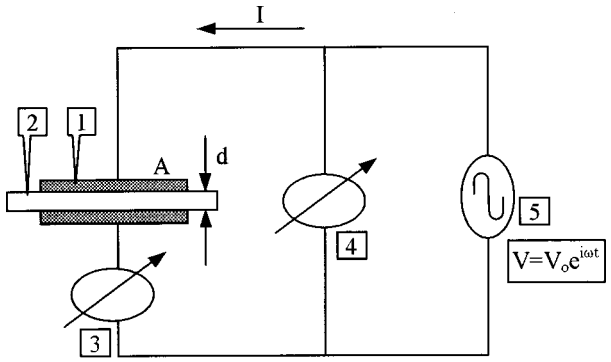

FIG. 1. Schematic view of a typical dielectric spectroscopy experiment. (1) Electrodes of area A, (2) sample film of thickness *d*, (3) current analyzer, (4) voltage analyzer, and (5) alternating voltage generator.

tained during the crystallization process from the glassy state of poly (ethylene terephthalate) (PET) which can be considered as a model crystallizable polymer.

II. DESCRIPTION OF THE EXPERIMENTAL SETUP FOR SIMULTANEOUS MEASUREMENT OF WAXS, SAXS, AND DS

Generally, the dielectric spectroscopy technique measures the complex dielectric permittivity $\epsilon^* = \epsilon' - i\epsilon''$ as a function of frequency and temperature, where ϵ' is the dielectric constant and ϵ'' is the dielectric loss. A schematic view of a dielectric spectroscopy experiment is shown in Fig. 1. A dielectric sample of thickness d and area A is subjected to an alternating electric field of angular frequency ω. Through measurements of the complex impedance of the sample it is possible to experimentally determine ϵ^*.[13] Dielectric spectroscopy is a very suitable method to study molecular dynamics in polymers above T_g. In this case, segmental motions of the polymeric chains give rise to the so called α-relaxation process, which can be observed as a maximum in ϵ'' and a step-like behavior in ϵ' as a function of frequency as illustrated in Fig. 2(a) for PET and in Fig. 2(b) for a copolymer of poly (hydroxybutyrate) and poly(hydroxyvalerate) P(HB)–co–P(HV) (78/22). Both, the intensity of the α relaxation, $\epsilon''_{\max}$, and the frequency of maximum loss $F_{\max}$ are very sensitive to crystallinity, which produces a decrease in $\epsilon''_{\max}$ and a shift of $F_{\max}$ towards lower values when crystallization proceeds.[9–12]

A scheme of the SAXS–WAXS–DS sample holder, to be called SWD, is illustrated in Fig. 3. Sample (1) is placed between two metallic disks (3) (3 cm diameter) acting as electrodes. These are electrically insulated by polyamide films (5) from the heating blocks (4). Heating power is provided by four cartridge heating-elements (6) (Watlow ''firerod,'' 100 W each) embedded in the sample-cell heating blocks (4). In order to allow the passage of the x-ray beam through the sample, central holes were machined in both, the electrodes and in the heating blocks (see Fig. 3). The sample, prepared in the form of a film, is provided with circular gold electrodes (3 cm diameter) by sputtering the metal in both free surfaces. The sample film was sandwiched between two thin aluminum disks (2) (0.01 cm thick) in order to provide homogeneous heating for the whole sample surface. The

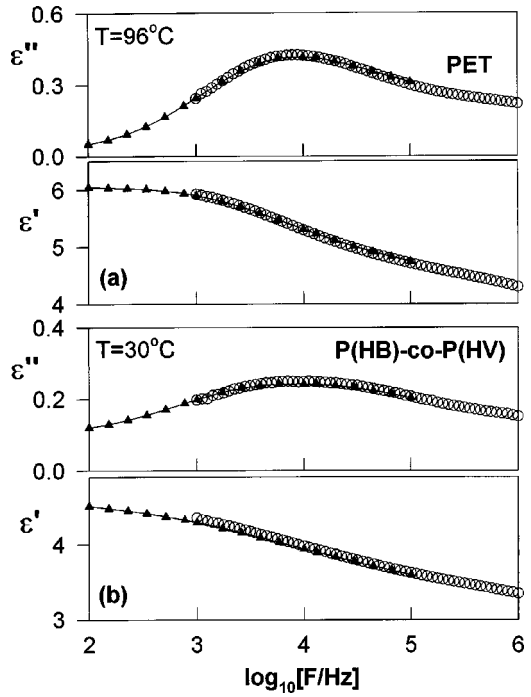

FIG. 2. Dielectric loss, ϵ'', and dielectric constant, ϵ', as a function of frequency, $F = \omega/(2\pi)$, for (a) amorphous PET at $T = 96\,^{\circ}\mathrm{C}$ and (b) semicrystalline P(HB)–co–P(HV) copolymer at $T = 30\,^{\circ}\mathrm{C}$. Solid symbols: measurement performed with a NOVOCONTROL equipment, open symbols: SWD experimental data.

sandwich is placed in between the two metallic electrodes (3). Cooling of the device can be obtained by compressed air circulating through a metallic pipe (7) embedded in one of the sample-cell heating blocks. Temperature control is provided by a Watlow series 96 closed-loop temperature controller achieving a temperature accuracy of $\pm 0.25\,^{\circ}\mathrm{C}$. A thermometer (8) (PT-100, three wire connection setup) was located in one of the metallic electrodes. Electrodes are connected to a Hewlett-Packard impedance analyzer HP 4192A allowing to measure dielectric complex permittivity (ϵ^*) in the 10^3–10^6 Hz frequency range. Although other type of im-

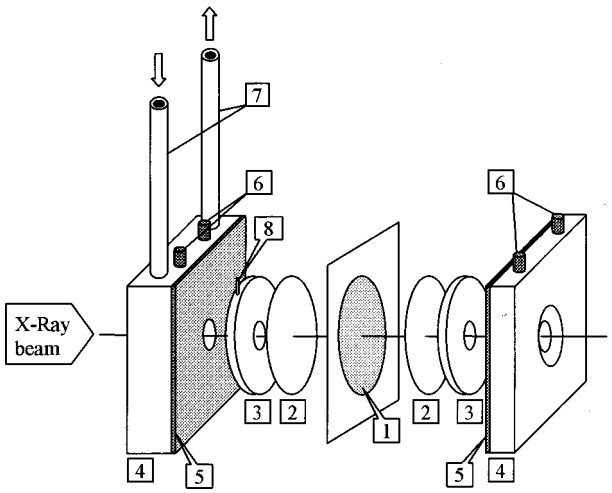

FIG. 3. Scheme of the SAXS–WAXS–DS cell. (1) Sample, (2) aluminum disks, (3) electrodes, (4) heating blocks, (5) insulating polyamide film, (6) heating elements, (7) cooling pipes, and (8) PT-100 thermometer.

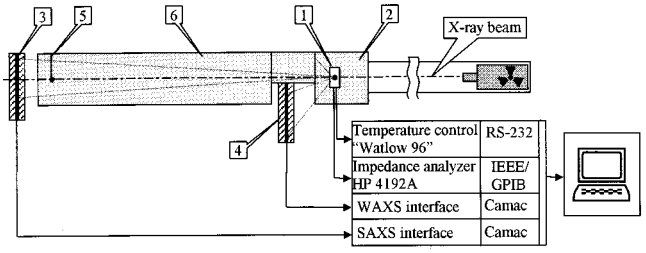

FIG. 4. Scheme of the experimental setup for simultaneous SAXS–WAXS–DS experiments at polymer beam line A2 at HASYLAB–DESY. (1) SAXS–WAXS–DS sample cell, (2) vacuum chamber, (3) SAXS detector, (4) WAXS detector, (5) Beam stop, and (6) vacuum evacuated optical path.

pedance analyzers, lock-in amplifiers or dielectric analyzers are also suitable for conventional dielectric spectroscopy,[14] we choose the earlier mentioned one in order to reduce the data acquisition time over the three frequency decades to be lower than 30 s. This assures the performance of dielectric measurements during crystallization in real time.[11,12] In order to test the performance of the SWD cell measurements were accomplished in different polymers by using a commercial dielectric spectrometer (Novocontrol BDS 810). Results were compared to those obtained by the SWD cell and are shown in Fig. 2 for (a) PET and (b) P(HB)–co–P(HV).[15] As one sees, the agreement between both measurements is satisfactory.

The SWD cell is incorporated into a vacuum chamber specially designed to perform x-ray scattering measurements with synchrotron radiation. Simultaneous SAXS, WAXS, and DS experiments were performed in the Polymer beam line at HASYLAB (DESY) in Hamburg by using the device designed by Bark and Zachmann.[8] A scheme of such a device incorporating the SWD cell is presented in Fig. 4. This system uses two position sensitive Gabriel detectors. Closer to the sample, the WAXS detector (4) is positioned off the primary beam allowing the SAXS intensity to pass above and to be measured by the SAXS detector (3) located at a larger distance (2.35 m). The complete optical path (6) is under rotatory pump vacuum. X-ray scattering data are corrected for fluctuations in the intensity of the primary beam and background. The x-ray data can be taken with different accumulation times by using an acquisition system based on CAMAC hardware and modulator software.[16] The DS data taken by the dielectric analyzer are collected by an IEEE-interface interconnected with a PC.

III. SIMULTANEOUS SAXS, WAXS, AND DS MEASUREMENTS DURING CRYSTALLIZATION OF A MODEL POLYMER: PET

In order to test the performance of the SWD cell, we selected a commercial sample of PET (Rhodia S80 from RhodiaSter-Rhoune Poulenc) which is considered as a suitable model polymer for the study of polymer crystallization.[10] A glassy PET specimen was obtained by press molding and quenching of the original sample in ice water from the molten state. PET, like many other glassy polymers, can develop a certain degree of crystallinity provided it is heated at $T > T_g = 75\,^{\circ}\mathrm{C}$. Figure 5 presents SAXS–WAXS–DS data during a crystallization experiment at $T_c = 116\,^{\circ}\mathrm{C}$ taken in a simultaneous fashion for different crystallization times t_c. The SAXS(a), and WAXS(b) intensities are given as a function of the scattering vector $s = (2/\lambda)\sin\theta$, 2θ being the scattering angle. Every pattern was recorded with an acquisition time of 1 min. The ϵ'' data from DS are presented as a function of frequency [$F = \omega/(2\pi)$]. The initial amorphous state, $t_c = 1$ min, is characterized by an amorphous halo in the WAXS diagram, a continuous scattering decreasing with s in the SAXS pattern, due to the liquid-like state, and by the presence of the α relaxation process centered around a $F_{\max}$ value of 4×10^5 Hz in the DS data. The absolute error in ϵ'', represented in selected data for the sake of clarity, was obtained from an average over several experiments. As time increases, the onset of crystallization is denoted by the incipient appearance of Bragg peaks in the WAXS patterns centered around $s = 0.188$, $s = 0.\overline{2}02$, $s = 0.\overline{2}66$, and $s = 0.300\,\text{Å}^{-1}$ characteristics of the $0\bar{1}1$, 010, $1\bar{1}0$, and 100 reflections of the triclinic unit cell of PET. In the SAXS pattern it is observed an increase of the scattered scattering at lower s values that develops into a well defined peak centered around a value of $s = 0.01\,\text{Å}^{-1}$. The earlier mentioned structural features are accompanied by the changes in the dynamics of the amorphous phase [see Fig. 5(c)]. Here, the α relaxation exhibits with crystallization time a decrease of its intensity and a shift towards lower frequencies of $F_{\max}$.

A summary of the changes of the earlier mentioned characteristic magnitudes is presented in Fig. 6. The long period values (L) calculated from the Lorenz corrected SAXS intensity (Is^2),[5] the integrated intensity of the 100 peak (A_c) as described elsewhere,[15] and the Lorentz corrected integrated SAXS intensity (Q) are presented in the upper part of Fig. 6.

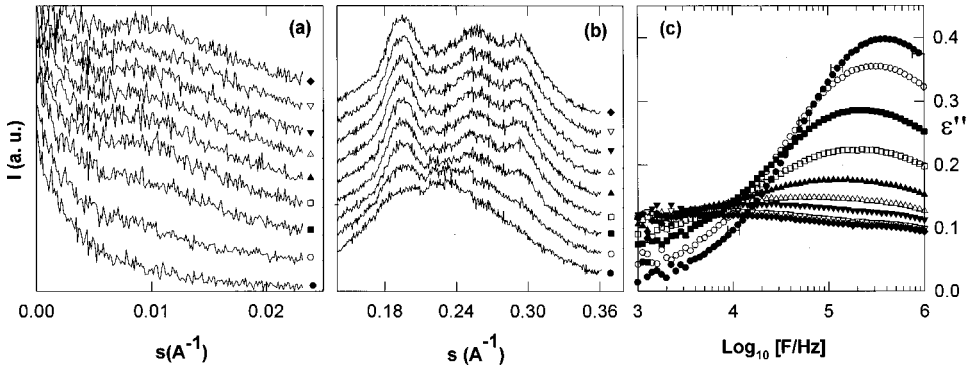

FIG. 5. Simultaneous SAXS (a), WAXS (b), and DS (c) experiment during crystallization of initially amorphous PET at $T_c = 116\,^{\circ}\mathrm{C}$. Different symbols correspond to different crystallization times: (●) $t_c = 1$, (○) $t_c = 5$, (■) $t_c = 10$, (□) $t_c = 15$, (▲) $t_c = 20$, (△) $t_c = 25$, (▼) $t_c = 30$, (▽) $t_c = 50$, and (◆) $t_c = 100$ min.

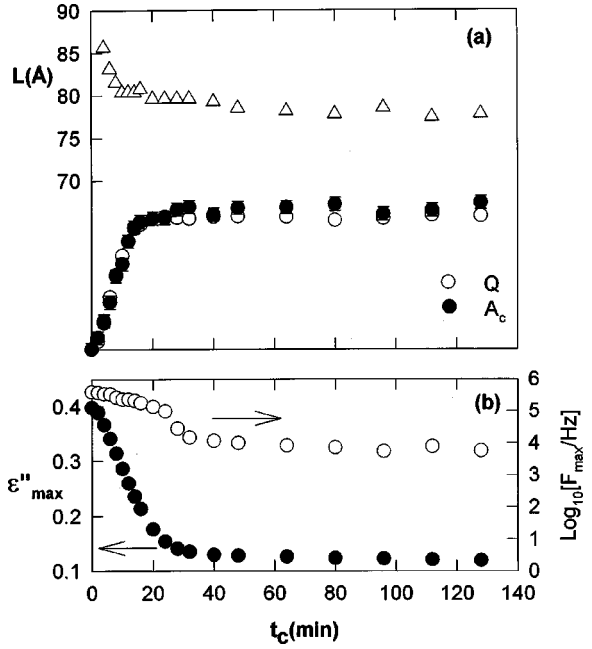

FIG. 6. Summary of physical magnitudes obtained from the SWD experiment. (a) Long spacing L (△), area of the characteristic reflection 100 A_c (●) and SAXS integrated intensity Q (○) as a function of crystallization time (t_c). (b) Maximum loss value ϵ''_{max} (●) and frequency of maximum loss F_{max} (○) as a function of t_c.

In the lower part, the characteristic parameters form the dielectric experiment (ϵ''_{max} and F_{max}) are also shown as a function of the crystallization time (t_c). As far as the x-ray scattering data is concerned, it is seen that for $t_c < 20$ min L significantly decreases and both, X_c and Q increase. This behavior is characteristic for the primary crystallization process[1,4] where spherulitic structures develop. At longer times, L, X_c, and Q slow down their time dependence. The latter behavior is characteristic of the secondary crystallization process where the spherulites already fill in the sample volume.[1,4] At this stage, crystallization may further proceed through other mechanism.[4] The earlier features provide information about changes occurring in the crystalline phase. In our experiment (using the SWD cell), this information can be complemented with that provided by the DS experiments which are sensitive to changes of the amorphous phase. On one hand, Fig. 6(b) shows that the intensity of the α relaxation initially decreases with t_c until about 20 min and subsequently remains constant. On the other hand, F_{max} slightly varies until $t_c = 20$ min and subsequently dramatically decreases reaching a plateau for longer times. This behavior is in agreement with previous dielectric experiments.[9,11] From the simultaneous SWD experiments a clear relationship between structure and dynamics emerges as evidenced by the following points: (i) the initial ($t_c < 20$ min) strong reduction of the mobile material reflected by the decrease on ϵ''_{max} parallels the increase of crystallinity and invariant Q, and the simultaneous decrease of long spacing. (ii) During this initial period, the remaining mobile material does not significantly change its dynamics as reflected by the moderate variation observed in F_{max}. (iii) At the crossover time $t_c \approx 20$ min, where primary crystallization finishes, F_{max} exhibits a notable decrease indicating the onset of restrictions in the dynamics of the remaining mobile fraction. The analysis of the experimental results obtained by the SWD technique on different polymers and crystallization conditions is in progress. The implication of the information obtained by this novel technique on the crystallization process of polymers will be the subject of a separate publication.[17]

ACKNOWLEDGMENTS

The authors are indebted to the DGICYT (Grant No. PB 94-0049) and to Comunidad de Madrid (07N/0063/1998), Spain, for generous support of this investigation. I. Šics thanks a AECI (Spain) for the tenure of a fellowship. A. N. thanks the support from the FPI program of the Spanish Ministry of Science and Culture (MEC). Z. D. thanks MEC for the tenure of a fellowship of the program ''Científicos y Tecnólogos Extranjeros.'' The experiments at HASYLAB (Hamburg, Germany) have been funded by the program Human Capital and Mobility, Access to large Installations EC (ERBFMGEDT 950059).

[1] J. M. Schultz, *Polymer Materials Science* (Prentice Hall, New York, 1974), p. 380.
[2] B. Wunderlich, *Macromolecular Physics* (Academic, New York, 1973), Vol. 1.
[3] P. J. Barham, in *Materials Science and Technology*, Structure and Properties of Polymers, Vol. 12, edited by R. W. Cahn, P. Haasen, and E. J. Kramer (VCH, Weinheim, 1993), p. 153.
[4] H. G. Zachmann and C. Wutz, in *Crystallization of Polymers*, edited by M. Dosiere (Kluwer Academic, Dordrecht, 1993), p. 403.
[5] F. J. Baltá-Calleja and C. G. Vonk, *X-ray Scattering of Synthetic Polymers* (Elsevier, Amsterdam, 1989), p. 241.
[6] C. Wutz, M. Bark, J. Cronauer, R. Döhrmann, and H. G. Zachmann, Rev. Sci. Instrum. **66**, 1303 (1995).
[7] H. G. Zachmann and R. Gehrke, in *Morphology of Polymers*, edited by B. Sedlàcek (Walter D. Gruyter, New York, 1986), p. 119.
[8] M. Bark and H. G. Zachmann, Acta Polym. **44**, 259 (1993).
[9] G. Williams, Adv. Polym. Sci. **33**, 59 (1979).
[10] J. C. Coburn and R. H. Boyd, Macromolecules **19**, 2238 (1986).
[11] T. A. Ezquerra, F. J. Baltá-Calleja, and H. G. Zachmann, Polymer **35**, 2600 (1994).
[12] T. A. Ezquerra, J. Majszczyk, F. J. Baltá-Calleja, E. López-Cabarcos, K. H. Gardner, and B. S. Hsiao, Phys. Rev. B **50**, 6023 (1994).
[13] A. R. Blythe, *Electrical Properties of Polymers* (Cambridge University Press, Cambridge, 1979).
[14] F. Kremer, D. Boese, G. Meier, and E. W. Fischer, Prog. Colloid Polym. Sci. **80**, 129 (1989).
[15] A. Nogales, T. A. Ezquerra, J. M. García, and F. J. Baltá-Calleja, J. Polym. Sci., Part B: Polym. Phys. **37**, 37 (1999).
[16] C. Boulin, R. Kempf, M. H. J. Koch, and S. M. Mclaughlin, Nucl. Instrum. Methods Phys. Res. A **249**, 399 (1986).
[17] I Šics, A. Nogales, T. Ezquerra, Z. Dentchev, and F. J. Baltá-Calleja (unpublished).